A study on differentiation of extra-cardiac activity by Slit Slat collimation in Single Photon Emission Computed Tomography

Original Article

Parvaneh Darkhor[1], Babak Mahmoudian[2], Esmaeil Gharepapagh[2], Seyed Rasoul Zakavi[3], Jalil Pirayesh Islamian[4]

[1]Immunology Research Center, Tabriz University of Medical Sciences, Tabriz, Iran
[2]Departments of Radiology, Tabriz University of Medical Sciences, Tabriz, Iran
[3]Nuclear Medicine Research Center, Mashhad University of Medical Sciences, Mashhad, Iran
[4]Departments of Medical Physics, Tabriz University of Medical Sciences, Tabriz, Iran

(Received 11 June 2017, Revised 12 October 2017, Accepted 14 October 2017)

ABSTRACT

Introduction: Myocardial perfusion SPECT by ^{99m}Tc-Sestamibi and ^{99m}Tc-Tetrofosmin radiopharmaceuticals usually presents a false significant increase in the radiotracer uptake in the inferior myocardium due to the uptake in organs such as liver, bowel, stomach and biliary system. The present study evaluated a suitable Slit angle for differentiating extra-cardiac activities by Slit Slat collimation.

Methods: The Siemens E.CAM gamma camera equipped with a Low Energy High Resolution (LEHR) collimator was simulated with the Simulating Medical Imaging Nuclear Detectors (SIMIND) Monte Carlo program. Following the verification of the simulation, a Slit Slat collimator was simulated for SPECT imaging of a NURBS-based Cardiac Torso (NCAT) phantom with different Slit angels ranged from 0 to 30 degrees. The reconstructed images were qualitatively assessed with blinded observer method by three nuclear medicine specialists.

Results: The improved differentiation of the bowel activity from the cardiac was obtained by a Slit-Slat collimator with the Slit angle of 7 degree. While for gastric activity differentiation an angle of 15 degree for the Slit was useful.

Conclusion: The results showed that Slit Slat collimation with 7 and 15 Slit angle provide a suitable differentiation of the bowel and gastric activities from the cardia, respectively.

Key words: Myocardium; NCAT; SPECT, Slit Slat collimator; SIMIND Monte Carlo

Iran J Nucl Med 2018;26(1):22-29
Published: January, 2018
http://irjnm.tums.ac.ir

Corresponding author: Dr. Jalil Pirayesh Islamian, Departments of Medical Physics, Tabriz University of Medical Sciences, Tabriz, Iran. E-mail: pirayeshj@gmail.com

INTRODUCTION

Myocardial perfusion SPECT (MPS) is widely used for the diagnosis of cardiac and coronary artery diseases [1-4]. Although ^{99m}Tc-Sestamibi (MIBI) and ^{99m}Tc-Tetrofosmin radiopharmaceuticals are generally utilized for myocardial perfusion imaging (MPI), but they do not meet the requirements of an ideal myocardial perfusion imaging radiopharmaceuticals, mainly due to unregistered uptake in sub diaphragmatic organs such as liver, stomach, biliary system and bowels [5-7].

The scattered radiation from the adjacent organs may cause a false uptake in the inferior wall of heart. Due to the high uptake of the radiopharmaceuticals in the liver and slow clearance, interpretation on the heart inferior and left ventricular wall activity is a critical issue on the reconstructed images with attenuation correction and maximum likelihood expectation maximization (MLEM) reconstruction [5, 8]. In a study by Brander horst et al., the effect of high tracer uptake of ^{99m}Tc-Tetrofosmin MPI was investigated in mice with a multi pinhole SPECT geometry [9]. The results showed that a high activity in extra-cardiac leads to an incorrect quantification of the organ uptake. This is an important challenge for a proper diagnosis of heart diseases [7, 10].

Peace et al. in a study on suitable radiopharmaceutical compounds and conservative protocols to reduce extra-cardiac activities were evaluated the effects of imaging time, radiopharmaceutical, full fat milk and water on interfering extra-cardiac activity in MPS [8]. One group of patients were imaged with both the Tetrofosmin or MIBI protocols at 0.5, 1, or 2 hour post injection. Other groups were imaged either with or without orally administration milk and a combination of milk with water. Although there was no significant improvement by using the latter, but the delayed imaging for Tetrofosmin and Sestamibi improved image interpretation. In a study by Hofman et al., the efficacy of milk administration compared to the water to reduce infra cardiac activity was assessed [11]. In contrast to the results of previous study, the intensity of infra cardiac activity was significantly reduced with milk rather than water in patients undergoing exercise or pharmacological stress. However, there was no difference in subsequent qualitative evaluation. Chen et al., have evaluated bio distribution of ^{99m}Tc-CO-MIBI as a myocardial perfusion imaging agent. Their study showed a significant concentration of ^{99m}Tc-CO-MIBI in myocardium with a lower liver uptake compared to ^{99m}Tc-sestamibi [5].

A number of researches have been working in the field of dedicated heart collimation [12, 13]. Conventionally, MPS is performed by a parallel hole collimator [1, 14, 15]. Growing interests in improving image quality and diagnostic accuracy had led to introduction of some novel collimator geometries in cardiac SPECT imaging [14, 16-18]. The IQ SPECT system (Siemens Medical Solutions) equipped with multifocal collimators, with the holes focused at center and parallel at edge, provide a better sensitivity (4-fold) and contrast-to-noise ratio than a parallel hole collimator [2]. IQ SPECT system was studied by Caobelli et al., to reduce the administered dose and acquisition time. The related rest scans of an anthropomorphic cardiac phantom were acquired with a simulated in vivo distribution of ^{99m}Tc-Tetrofosmin. Qualitative as well as quantitative measurements resulted a reduced acquisition time to one-eighth of the time needed with a standard protocol, also with a reduced administered radiopharmaceutical dose [2, 4, 19]. The Slit Slat collimation for cardiac imaging have become available in the dedicated scanners [20]. It was described for the first time as a part of the dedicated brain SPECT system [21]. CardiArc (a dedicated nuclear cardiology SPECT camera) equipped with an optimized Slit Slat collimation system provides an angular sampling via moving the Slit plate [14, 22, 23]. On the other hand, a Slit Slat design which incorporates a curved Slit plate and a stack of Slats parallel to the transverse plane was planned in a C-SPECT system and improved performance of cardiac SPECT imaging.

Here, the general objective of present research was to survey suitable Slit angle in SPECT to differentiate inferior heart activity from the sub-diaphragmatic organs by Slit Slat collimation. When orthogonal parallel hole collimator provides an overlapped extra-cardiac activities, a Slit Slat design was used to develop an angulated Slit toward cardiac region so that the optimal angulation may be provided suitable differentiation of the hyper cardiac activity from the underling organs. The hypothesis is further studied by employing a NURBS-based Cardiac Torso (NCAT) digitized phantom and Monte Carlo simulation.

METHODS

Imaging system

A dual head Siemens E.CAM gamma camera (Siemens Medical Solutions, Erlangen, Germany) was used for the simulation study. The camera includes a removable low energy high resolution (LEHR) parallel hexagonal holes collimator, a 59.1×44.5×0.953 cm NaI: Tl scintillation crystal, a light guide and also an array of Photomultiplier Tubes (65 PMTs).

Monte Carlo simulation

The SIMIND dedicated Monte Carlo simulation code was used for the simulation studies [24]. A LEHR parallel hole and also a Slit Slat collimator for the energy of 140 Kev were simulated with a 15% window width (Table 1) [25].

Table 1: Physical specification of SE-LEHR and Slit Slat collimator

Type	Slit width	Slat width	Hole diameter	Septal thickness	Collimator thickness
SE_LEHR	--	--	1.11mm	0.16mm	24.05mm
Slit Slat	1.11mm	1.24mm	--	0.16mm	24.05mm

The pixel sizes in the simulated point source, Jaszczak and NCAT phantoms were set to 0.27, 0.39, and 0.7 cm, respectively. The details on SPECT acquisition parameters for the Jaszczak phantom scans considered as following:

A 128×128 matrix size, 1 zoom factor, 128 projections, and 360° counter-clockwise circular rotation. Moreover, the SPECT studies on superimposed extra-cardiac activities in cardiac region were simulated by the simulated SPECT camera equipped with a Slit Slat collimation with Slit angles in range of 0-30 degrees. The concentration of ^{99m}Tc–MIBI in myocardium and extra-cardiac organs were simulated according to the clinical situation [26].

The SPECT imaging protocol for NCAT phantom studies was adopted from the last American Society of Nuclear Cardiology (ASNC) imaging guidelines for nuclear cardiology procedures [27].

Briefly, Thirty-two SPECT projections of the NCAT phantom, an average male torso in a supine position, were produced with a 180° clockwise rotation (+45° right anterior oblique to -45° left posterior oblique) in a 64×64 matrix size.

Phantoms

The experimental scans performed with a 1mm ^{99m}Tc point source (3.7 MBq) and a Jaszczak phantom (uniformly filled with 370 MBq ^{99m}Tc). According to the experiment and simulated scans, functional parameters of the both systems including spatial resolution, energy resolution and sensitivity were evaluated. Contrast of the cold spheres in reconstructed images of Jaszczak phantom was calculated by Eq.1 [28].

$$\text{Contrast} = 1 - (M_{sp} / M_{cy}) \qquad \text{Eq.1}$$

Where, M_{sp} and M_{cy} are the Min pixel value in cold spheres and Max pixel value in the phantom cylinder, respectively.

Additionally, the organ contrast of the NACT phantom reconstructed images was calculated by Eq.2 [29, 30].

$$\text{Contrast} = (A-B) / (A+B) \qquad \text{Eq.2}$$

Where A and B represent the average count in the myocardial wall and the extra-cardiac area, respectively.

Spatial resolution

Spatial resolution of the imaging system was measured by a ^{99m}Tc point source at 10 cm from the detector in the center field of view (CFOV) according to the NEMA standards [31]. The planar images were obtained with 10 million counts, matrix size of 128×128 with a 0.39 mm pixel size, for the both simulations and experiments. For quantifying FWHM values, a point spread function was prepared through the point source images.

The Jaszczak phantom filled with 370 MBq ^{99m}Tc solution was placed at 15 cm from the collimator surface. The spatial resolution measure was scored as the smallest visible and recognizable rods of the phantom.

Energy resolution

The energy resolution was measured by employing a ^{99m}Tc point source at a source to detector distance of 25 cm. The simulated and experimental energy spectra were acquired with 10^7 photons / projection.

System sensitivity

The system sensitivity was also calculated from a 3.7 MBq ^{99m}Tc point source planar data according to the NEMA [31].

Image reconstruction

The filtered back projection (FBP) algorithm [32] was utilized for reconstruction of the Jaszczak and NCAT phantom SPECT projections through a ramp combined with a Butterworth filter (order 5 and cut off frequency of 0.25 cycles/cm) and no attenuation correction [32, 33].

The evaluations on the extra-cardiac activity for the reconstructed images were independently done as a blinded observer study by three nuclear medicine physicians. The images scored for a proper separation of the cardiac activity in a range of 0-20 according to the organ proper activity separation.

RESULTS

Simulation verification

Figure 1 demonstrates energy spectra of the simulated and experimental systems from scan of a ^{99m}Tc point source for simulation verification propose. The related energy resolutions were calculated to 9.86 % and 10.05 %, respectively. Figure 2 shows full width at half maximum (FWHM) measures of the point spread function (PSF) curves with an upward trend following the increased source to collimator distances.

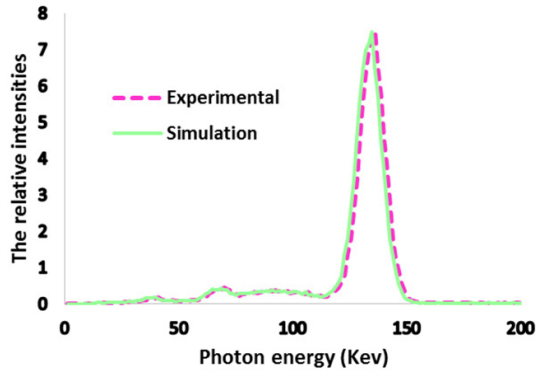

Fig 1. The normalized energy spectrum of the simulated and experimental systems.

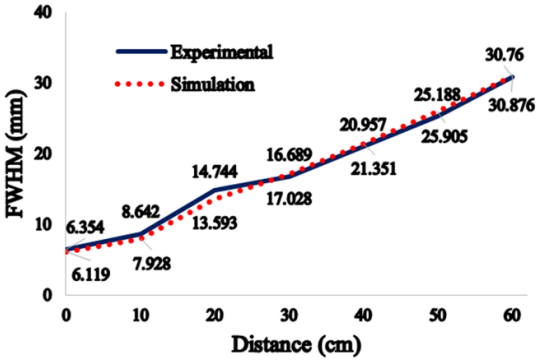

Fig 2. Comparison of FWHM as a function of distance for a ^{99m}Tc point source in the simulated and experimental systems.

The mean sensitivities of the experiment and simulation systems were determined 76.71 and 76.92 cps/MBq, respectively. The smallest visible and recognizable cold rods of the reconstructed Jaszczak phantom images were seen in the sector of 9.5 mm. Results on the contrast of cold spheres are shown in Table 2.

Slit Slat SPECT

A male NCAT phantom was set to model ^{99m}Tc-Sestamibi uptake study in myocardium and extra-cardiac organs. The SPECT imaging process simulated without any respiratory motion. A typical transaxial activity and attenuation distribution in NCAT phantom is shown in Figure 3.

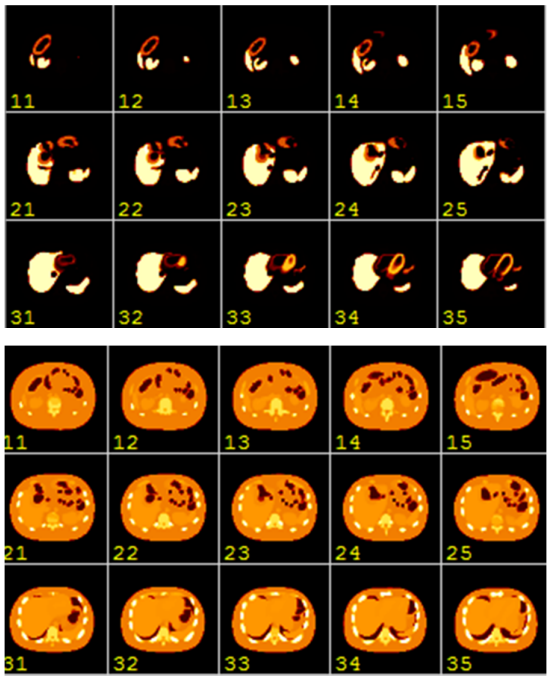

Fig 3. The simulated maps with NCAT phantom; the activity map (above) and the attenuation map (below).

Table 2: Contrast results for cold spheres of Jaszczak phantom.

Systems	Diameter size of spheres (mm)					
	9.5	12.7	15.9	19.1	25.4	31.8
Simulation	0.471	0.531	0.672	0.706	0.843	0.938
Actual	0.411	0.558	0.684	0.717	0.825	0.894

Table 3: The extra-cardiac activity differentiation in scoring process.

Slit angle (degree)	Image No	Specialist 1	Specialist 2	Specialist 3
5	K5G23	12.5	11	12
	K5G31	12	11	11
6	K6G23	15	15	15
	K6G31	18	15	16
7	K7G23	20	20	20
	K7G31	16	15	13
8	K8G23	17	18	18
	K8G31	14	12	13
9	K9G23	20	20	19
	K9G31	14	15	14
10	K10G23	12.5	14	15
	K10G31	14	13	13
11	K11G23	12.5	14	15
	K11G31	18	15	16
12	K12G23	15	13	14
	K12G31	18	16	16
13	K13G23	15	15	14
	K13G31	16	15	16
14	K14G23	17	15	14
	K14G31	16	17	17
15	K15G23	15	15	14
	K15G31	20	20	19

The reconstructed NCAT SPECT images prepared with a LEHR parallel hole collimation was considered as the reference. The simulated SPECT images by the Slit Slat collimator in various Slit angles were compared with the reference images. The results on intr-observer differences in scoring the extra-cardiac activity differentiation with visual assessment process are presented in Table 3. The image numbers with G23 and G31 are related to the bowel and gastric extra-cardiac activities, respectively.

Table 4 demonstrates a ratio of the cardiac wall contrast to extra cardiac activity, by means of HLA view and mean value of the counts through the plotted ROIs. The sensitivity and contrast for the Slit Slat collimation with a 7 degree Slit angle were increased to 1.02% and 1.86%, respectively.

Table 4: The quantitative parameters for simulated scans.

Hole angle of collimator	Sensitivity (Cps/MBq)	Relative contrast
Parallel hole	18.9961	0.1479
Slit slat (1˚)	18.9866	0.1465
Slit slat (2˚)	18.9925	0.1521
Slit slat (3˚)	18.9760	0.1590
Slit slat (4˚)	18.9655	0.1729
Slit slat (5˚)	18.9318	0.2795
Slit slat (6˚)	19.6005	0.2410
Slit slat (7˚)	19.5556	0.2754
Slit slat (8˚)	19.9055	0.2705
Slit slat (9˚)	20.3300	0.2812
Slit slat (10˚)	20.2793	0.2578

DISCUSSION

We have simulated a LEHR parallel hole and a Slit Slat collimator with different Slit angles for a SPECT system to measure the effects of the collimators on differentiation of the activities of heart and subdiaphragmatic organs. The conformity on functional parameters of the simulated and experimental systems have already been described for Siemens E.cam gamma camera equipped with a LEHR collimator [28]. As Figure 1 shows, there was a suitable compliance for the normalized energy spectra of the ^{99m}Tc point source scans from the simulated and experimental systems. The spatial resolution for experiment and simulated systems was measured 8.64 and 7.92 mm, respectively.

Separate simulations were also made to allow the investigation on extra-cardiac activities in several organs consisting of stomach and bowel for a wide range of Slit angles (0-30 degrees). The results of our study support the theoretical advantages of using an angulated collimator for differentiating extra-cardiac activities. Here, we demonstrated that a Slit Slat collimator with a suitable Slit angle can improve differentiation of the superimposed activities. In fact, angulating of Slit plate provided all of the required angular sampling. The theoretical advantages of using an angulated collimator has been supported in Esser et al. study for cranial SPECT imaging [34].

In addition to the simulated scans with LEHR parallel hole collimator, a lower Slit angles (1-3 degree) also presented the highest amount of the overlapped extra-cardiac activities (Figure 4). This is probably related to the anatomical orientation of the organs and the fact that the higher Slit angles are so needed to differentiate the activities. Results on scoring the proper activity differentiation by physicians demonstrated that the simulated scans with 7 degree of the Slit angle could properly differentiate the bowel activity from the cardiac (Figure 5).

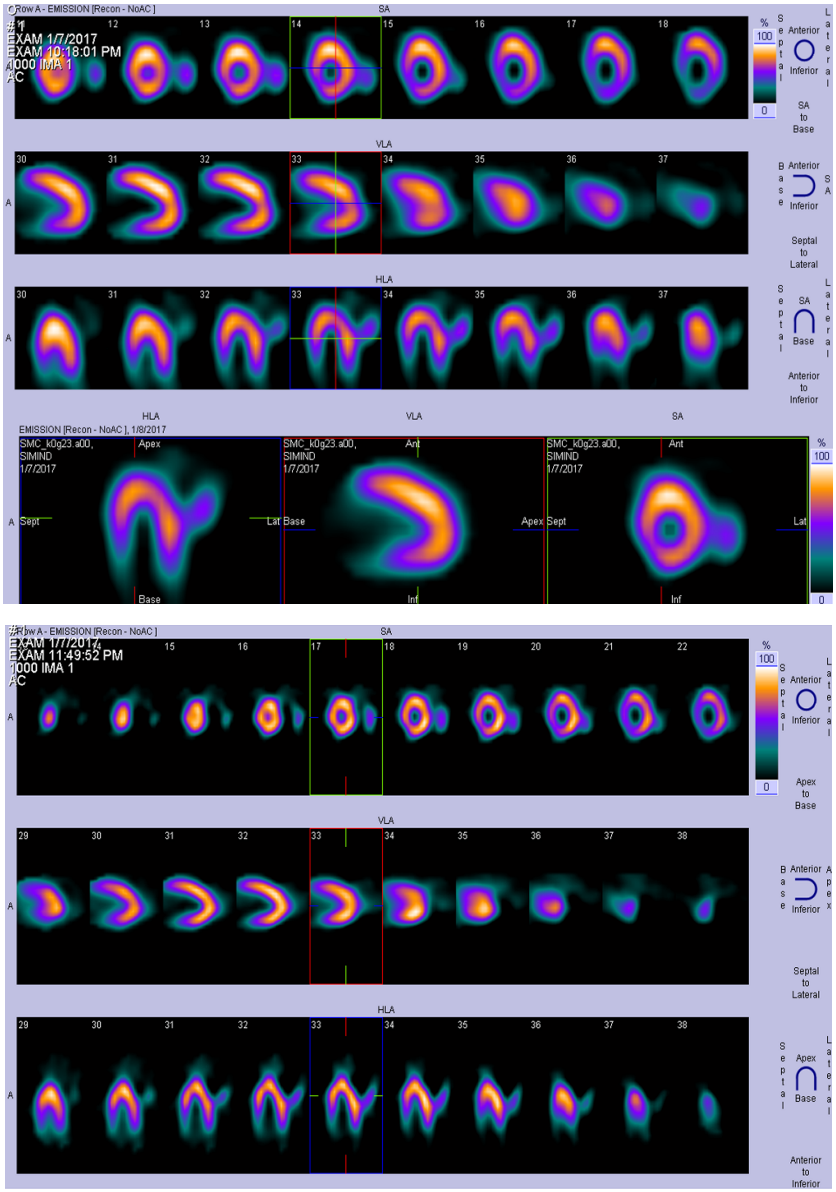

Fig 4: The reconstructed images equipped with; parallel hole collimation (above) and 7 degree of Slit angle to differentiate bowel extra-cardiac activity and heart (below).

Sheng proposed an elliptical SPECT system with Slit Slat collimation in which multiple Slits were designed for cardiac imaging [35]. The angular sampling was done by moving of the Slit plate. The differences in their angular sampling study and our study correlated with corresponding differences in collimation geometries (multi Slit hole versus Slit hole collimation).

The results on comparing quantitative parameters (Table 3) demonstrated a higher sensitivity and contrast ratio for the Slit angles above 6 degree than the conventional parallel hole collimation and confirmed the results on improved sensitivity with Slit Slat collimation for cardiac imaging by Sheng [35].

A proper gastric activity differentiation from cardiac was obtained with a 15 degree Slit angle (Figure 5). Due to heart asymmetric orientation, the angular sampling with the Slit angles more than 16 degree causes an insufficient activity concentration in cardiac region and also sever deformation of the organ image. One of the limitations about Slit Slat collimation in the present study was a linear distortion. Because more of the organ face the camera along the angulated dimension, the sensitivity increases, but the organ is

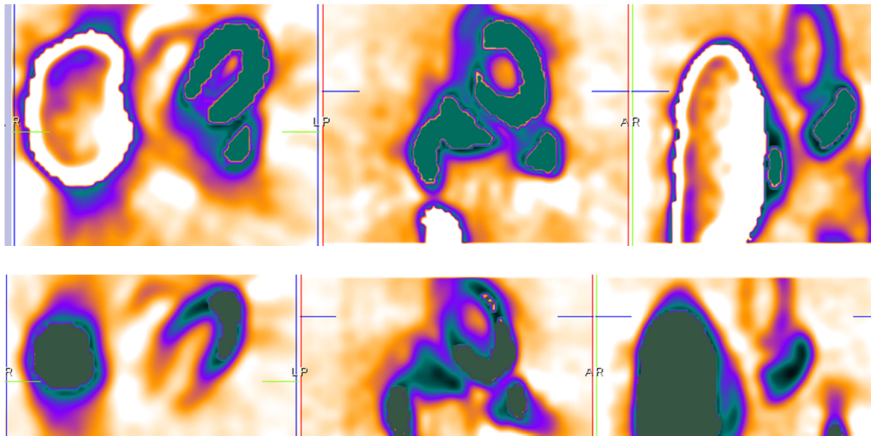

Fig 5. The reconstructed images equipped with; parallel hole collimation (above) and 15 degree of Slit angle (below) to differentiate gastric extra-cardiac activity and heart.

also elongated directionally in the image. Therefore, we conclude that Slit angles above 16 degree is restricted by the transaxial sampling requirements. Finally, physicians identified an artifact in the projections and in the reconstructed images that may be associated to the appearance of shadows from the Slats [17]. The results revealed that the effect of the extra-cardiac activities may be decreased from cardiac region by angulating of the Slit within a heart area in Slit Slat collimation geometry.

CONCLUSION

The present study suggested that the collimation with a Slit angle of 7 and also with 15 degree may provide the best differentiation of the bowel and gastric extra-cardiac activities from cardiac in Slit Slat collimation geometry, respectively.

Acknowledgments

The authors would like to express their appreciation to the staff of Nuclear Medicine Department in Imam Reza Hospital of Tabriz university of Medical Sciences for their sincere collaboration. This study was financially supported by the Immunology Research Center in Tabriz university of Medical Sciences (Grant number: 94/126), Tabriz, Iran.

REFERENCES

1. Liu C, Xu J, Tsui BM. Myocardial perfusion SPECT using a rotating multi-segment slant-hole collimator. Med Phys. 2010 Apr;37(4):1610-8.
2. Caobelli F, Kaiser SR, Thackeray JT, Bengel FM, Chieregato M, Soffientini A, Pizzocaro C, Savelli G, Galelli M, Guerra UP. IQ SPECT allows a significant reduction in administered dose and acquisition time for myocardial perfusion imaging: evidence from a phantom study. J Nucl Med. 2014 Dec;55(12):2064-70.
3. Armstrong IS, Saint KJ, Tonge CM, Arumugam P. Evaluation of general-purpose collimators against high-resolution collimators with resolution recovery with a view to reducing radiation dose in myocardial perfusion SPECT: A preliminary phantom study. J Nucl Cardiol. 2017 Apr;24(2):596-604.
4. Onishi H, Matsutomo N, Kangai Y, Saho T, Amijima H. Differential impact of multi-focus fan beam collimation with L-mode and conventional systems on the accuracy of myocardial perfusion imaging: Quantitative evaluation using phantoms. Asia Ocean J Nucl Med Biol. 2013 Fall;1(2):28-34.
5. Chen X, Guo Y, Zhang Q, Hao G, Jia H, Liu B. Preparation and biological evaluation of 99mTc-CO-MIBI as myocardial perfusion imaging agent. J Organomet Chem. 2008;693(10):1822-8.
6. Rojas G, Raff U, Gonzalez P, Jaimovich R, Quintana JC. Semi-automated assessment of left ventricular mass using transaxial Tc-99m Sestamibi SPECT imaging. Comput Med Imaging Graph. 2009 Jun;33(4):247-55.
7. Kim YS, Wang J, Broisat A, Glover DK, Liu S. Tc-99m-N-MPO: novel cationic Tc-99m radiotracer for myocardial perfusion imaging. J Nucl Cardiol. 2008 Jul-Aug;15(4):535-46.
8. Peace RA, Lloyd JJ. The effect of imaging time, radiopharmaceutical, full fat milk and water on interfering extra-cardiac activity in myocardial perfusion single photon emission computed tomography. Nucl Med Commun. 2005 Jan;26(1):17-24.
9. Branderhorst W, van der Have F, Vastenhouw B, Viergever MA, Beekman FJ. Murine cardiac images obtained with focusing pinhole SPECT are barely influenced by extra-cardiac activity. Phys Med Biol. 2012 Feb 7;57(3):717-32.
10. Adamson K. Principles of myocardial SPECT imaging. In: Movahed A, Gnanasergaran G, Buscombe J, Hall M, editors. Integrating cardiology for nuclear medicine physicians. Springer Berlin Heidelberg, Berlin, Germany; 2009. p.191-211.

11. Hofman M, McKay J, Nandurkar D. Efficacy of milk versus water to reduce interfering infra-cardiac activity in 99mTc-sestamibi myocardial perfusion scintigraphy. Nucl Med Commun. 2006 Nov;27(11):837-42.

12. Afzelius P, Henriksen JH. Extra cardiac activity detected on myocardial perfusion scintigraphy after intra-arterial injection of 99mTc-MIBI. Clin Physiol Funct Imaging. 2008 Sep;28(5):285-6.

13. Gholamrezanezhad A, Moinian D, Eftekhari M, Mirpour S, Hajimohammadi H. The prevalence and significance of increased gastric wall radiotracer uptake in sestamibi myocardial perfusion SPECT. Int J Cardiovasc Imaging. 2006 Jun-Aug;22(3-4):435-41.

14. Smith MF. Recent advances in cardiac SPECT instrumentation and system design. Curr Cardiol Rep. 2013 Aug;15(8):387.

15. Dehestani N, Sarkar S, Ay MR, Sadeghi M, Shafaei M. Comparative assessment of rotating slat and parallel hole collimator performance in GE DST-Xli gamma camera: A Monte Carlo study. In: Vander Sloten J, Verdonck P, Nyssen M, Haueisen J (eds). 4th European Conference of the International Federation for Medical and Biological Engineering. IFMBE Proceedings. Springer, Berlin, Heidelberg. 2009; 22:1062-65.

16. Bal G, Clackdoyle R, Kadrmas DJ, Zeng GL, Christian PE. Evaluating rotating slant-hole SPECT with respect to parallel hole SPECT. IEEE Nucl Sci Symp Med Imag Conf. 2000;22:67-71.

17. Metzler SD, Accorsi R, Novak JR, Ayan AS, Jaszczak RJ. On-axis sensitivity and resolution of a slit-slat collimator. J Nucl Med. 2006 Nov;47(11):1884-90.

18. Cao L, Peter J. Slit-slat collimator equipped gamma camera for whole-mouse SPECT-CT imaging. IEEE Trans Med Imaging. 2012;59:530-6.

19. Caobelli F, Thackeray JT, Soffientini A, Bengel FM, Pizzocaro C, Guerra UP. Feasibility of one-eighth time gated myocardial perfusion SPECT functional imaging using IQ-SPECT. Eur J Nucl Med Mol Imaging. 2015 Nov;42(12):1920-8.

20. Chang W, Ordonez CE, Liang H, Li Y, Liu J. C-SPECT - a clinical cardiac SPECT/Tct platform: Design concepts and performance potential. IEEE Trans Nucl Sci. 2009 Oct 6;56(5):2659-2671.

21. Rogers WL, Clinthorne NH, Stamos J, Koral KF, Mayans R, Keyes JW, Williams JJ, Snapp WP, Knoll GF. SPRINT: A stationary detector single photon ring tomograph for brain imaging. IEEE Trans Med Imaging. 1982;1(1):63-8.

22. DePuey EG. Advances in SPECT camera software and hardware: currently available and new on the horizon. J Nucl Cardiol. 2012 Jun;19(3):551-81; quiz 585.

23. Slomka PJ, Patton JA, Berman DS, Germano G. Advances in technical aspects of myocardial perfusion SPECT imaging. J Nucl Cardiol. 2009 Mar-Apr;16(2):255-76.

24. Ljungberg M, Strand SE, King MA. The SIMIND Monte Carlo program. Monte Carlo calculations in nuclear medicine: Applications in diagnostic imaging. Taylor & Francis; 2012.

25. Kau D, Metzler SD. Finding optimized conditions of slit-slat and multislit-slat collimation for breast imaging. IEEE Trans Nucl Sci. 2012;59:62-9.

26. Ghaly M, Du Y, Fung GS, Tsui BM, Links JM, Frey E. Design of a digital phantom population for myocardial perfusion SPECT imaging research. Phys Med Biol. 2014 Jun 21;59(12):2935-53.

27. Holly TA, Abbott BG, Al-Mallah M, Calnon DA, Cohen MC, DiFilippo FP, Ficaro EP, Freeman MR, Hendel RC, Jain D, Leonard SM, Nichols KJ, Polk DM, Soman P; American Society of Nuclear Cardiology. Single photon-emission computed tomography. J Nucl Cardiol. 2010 Oct;17(5):941-73.

28. Bahreyni Toossi MT, Islamian JP, Momennezhad M, Ljungberg M, Naseri SH. SIMIND Monte Carlo simulation of a single photon emission CT. J Med Phys. 2010 Jan;35(1):42-7.

29. Kalantari F, Rajabi H, Yaghoobi N. Optimized energy window configuration for 201Tl imaging. J Nucl Med Technol. 2008 Mar;36(1):36-43.

30. Saad IE, Helal NL, El-Din HM, Moneam RA. Evaluation of varying acquisition parameters on the image contrast in spect studies. Int J Res Rev Appl Sci. 2012;13:485-91.

31. NEMA NU 1-2012 Performance Measurements of Gamma Cameras. The National Electrical Manufactures Association (NEMA). 2012.

32. Piccinelli M, Garcia EV. Advances in software for faster procedure and lower radiotracer dose myocardial perfusion imaging. Prog Cardiovasc Dis. 2015 May-Jun;57(6):579-87.

33. Yussoff MS, Zakaria A. Relationship between the optimum cut off frequency for Butterworth filter and lung-heart ratio in 99mTc myocardial SPECT. Iran J Radiat Res. 2010;8:17-24.

34. Esser PD, Alderson PO, Mitnick RJ, Arliss JJ. Angled-collimator SPECT (A-SPECT): an improved approach to cranial single photon emission tomography. J Nucl Med. 1984 Jul;25(7):805-9.

35. Sheng J. An elliptical SPECT system with slit-slat collimation for cardiac imaging. Comput Med Imaging Graph. 2011 Jan;35(1):9-15.